Received 4 February 1997; accepted 1 July 1997.

1. Lewin, W. H. G., van Paradijs, J. & van den Heuvel, E. (eds) *X-ray Binaries* (Cambridge Univ. Press, 1995).
2. Alpar, M. A., Cheng, A. F., Ruderman, M. A. & Shaham, J. A new class of radio pulsars. **300,** 728–730 (1982).
3. Lyne, A. G. *et al*. The discovery of a millisecond pulsar in the globular cluster M28. *Nature* **328,** 399–401 (1987).
4. Saito, Y. *et al*. Detection of magnetospheric X-ray pulsations from the millisecond pulsar B1821–24. *Astrophys. J.* **477,** L37–L40 (1997).
5. Trumper, J. ROSAT. *Phys. Scripta T* **7,** 209–215 (1984).
6. Johnston, H. M., Verbunt, F. & Hasinger, G. ROSAT PSPC observations of globular clusters. *Astron. Astrophys.* **289,** 763–774 (1994).
7. Danner, R., Kulkarni, S. R. & Thorsett, S. E. ROSAT observations of six millisecond pulsars. *Astrophys. J.* **436,** L153–L156 (1994).
8. Tanaka, Y., Inoue, H. & Holt, S. S. The X-ray astronomy satellite ASCA. *Publ. Astron. Soc. Jpn* **46,** L37–L41 (1994).
9. Hasinger, G. *et al*. A deep X-ray survey in the Lockman hole and the soft X-ray log N – log S. *Astron. Astrophys.* **275,** 1–5 (1993).
10. Almaini, O. *et al*. A deep ROSAT survey. 12. The X-ray-spectra of faint ROSAT sources. *Mon. Not. R. Astron. Soc.* **282,** 295–303 (1996).
11. Rees, R. F. & Cudworth, K. M. A new look at the globular cluster M28 *Astron. J.* **102,** 152–158 (1991).
12. Krockenberger, M. & Grindlay, J. E. Discovery of diffuse X-ray emission in 47-tucanae. *Astrophys. J.* **451,** 200–209 (1995).
13. Kulkarni, S. R., Goss, W. M., Wolszczan, A. & Middleditch, J. Deep radio synthesis images of globular clusters. *Astrophys. J.* **363,** L5–L8 (1990).
14. Pacholczyk, A. G. *Radio Astrophysics* Ch. 7 (Freeman, San Francisco, 1970).
15. Foster, R. S., Backer, D. C., Taylor, J. H. & Goss, W. M. Period derivative of the millisecond pulsar in the globular cluster M28. *Astrophys. J.* **326,** L13–L15 (1988).
16. Verbunt, F., van Paradijs, J. & Elson, R. X-ray sources in globular clusters. *Mon. Not. R. Astron. Soc.* **210,** 899–914 (1984).
17. Hasinger, G., Johnston, H. M. & Verbunt, F. Discovery of multiple X-ray sources in 47-Tucanae. *Astron. Astrophys.* **288,** 466–471 (1994).
18. Grindlay, J. E. *et al*. Spectroscopic identification of probable cataclysmic variables in the globular cluster NGC-6397. *Astrophys. J.* **455,** L47–L50 (1995).
19. Asai, K. *et al*. ASCA observations of soft X-ray transients in quiescence—X1608-52 and Cen X-4. *Publ. Astron. Soc. Jpn* **48,** 257–263 (1996).
20. David, L. P., Harnden, F. R., Kearns, K. E. & Zombeck, M. V. in *The ROSAT High Resolution Imager Calibration Report* 1–52 (SAO, Cambridge, MA, 1996).
21. Djorgovski, S. & Meylan, G. in *Structure and Dynamics of Globular Clusters* (eds Djorgovski, S. G. & Meylan, G.) 325–336 (Astron. Soc. Pacif., San Francisco, 1993).
22. Trager, S. C., Djorgovski, S. & King, I. R. in *Structure and Dynamics of Globular Clusters* (eds Djorgovski, S. G. & Meylan, G.) 347–355 (Astron. Soc. Pacif., San Francisco, 1993).
23. Cognard, I. *et al*. High precision timing observations of the millisecond pulsar PSR B1821–24 at Nancy. *Astron. Astrophys.* **311,** 179–188 (1996).
24. Buccheri, R. & De Jaeger, O. C. in *Timing Neutron Stars* (eds Ögelman, H. & van den Heuvel, E. P. J.) 95–111 (Kluwer, Dordrecht, 1989).

Acknowledgements. We thank J. Grindlay and F. Verbunt for discussions. R.M.D. and S.R.K. thank NASA for support. This work was partially supported by the Scientific Research Fund of the Japanese Ministry of Education, Science, and Culture.

Correspondence should be addressed to S.R.K. (e-mail: srk@astro.caltech.edu).

Turbulent drag reduction by passive mechanisms

L. Sirovich & S. Karlsson

Orlev Scientific/Ormat Industries, PO Box 68, Yavne, 70650 Israel, and The Division of Engineering, Brown University, Providence, Rhode Island 02912, USA

In many situations involving flows of high Reynolds number (where inertial forces dominate over viscous forces), such as aircraft flight and the pipeline transportation of fuels, turbulent drag is an important factor limiting performance. This has led to an extensive search for both active and passive methods for drag reduction[1]. Here we report the results of a series of wind-tunnel experiments that demonstrate a passive means of effectively controlling turbulence in channel flow. Our approach involves the introduction of specified patterns of protrusions on the confining walls, which interact with the coherent, energy-bearing eddy structures in the wall region, and so influence the rate at which energy is dissipated in the turbulent flow. We show that relatively small changes in the arrangement of these protrusions can alter the response of the system from one of drag decrease to increased mixing (drag enhancement).

Experiments were carried out in a fully developed turbulent channel flow of half-height $h = 2.815$ cm, width 75 cm and length 8.5 m. (A description of the channel may be found elsewhere[2].) the range of Reynolds numbers (Re) of the channel, based on centre-line velocity, U_0, was $1.5 \times 10^4 < \mathrm{Re} = U_0 2h/\nu < 4 \times 10^4$, where ν is the kinematical viscosity. The flow therefore falls into the realm of fully developed turbulence downstream of the entry region[3]. By convention, such turbulent flows are viewed as having a central core flow which is referred to as the outer region, in contrast with the layer adjacent to the wall, referred to as the inner region. In the former region the characteristic length scale is the channel half-height h which, with U_0, defines a 'turnover' timescale, $\tau_0 = h/U_0$. Both h and τ_0 represent estimates of scales over which correlations are lost. Further, in the outer region viscosity plays an asymptotically small role and the mean velocity, $U(y)$, scales as $U_0 - U(y) = U_0 f(y/h)$, where y is the wall-normal distance. The inner velocity scale is the friction velocity, u_*, defined by the wall friction, $u_*^2 = \nu[\partial U/\partial y]_{y=0}$. The inner length scale is then given by $l_* = \nu/u_*$, and the mean velocity scales as $U(y)/u_* = g(y/l_*) = g(y_*)$, referred to as the law of the wall. u_* defines a second Reynolds number, $\mathrm{Re}_* = u_* h/\nu$, on which basis $750 < \mathrm{Re}_* < 2{,}000$ in our experiments.

Both $f(y/h)$ and $g(y_*)$ are regarded as being universal functions. Postulation of an overlap region[4,5] leads to the 'log-law', $U/u_* = \kappa^{-1} \ln y_* + B$ where κ, the von Karman constant, and B are empirically determined. Evidence of the log-law, in an investigation of pipe flow over three decades of Re (ref. 6), indicates a logarithmic overlap region at high Re (ref. 7).

Several features of the flow show universality. In particular fluctuations in the direction of the flow (u_{rms}) and turbulence production ($\overline{-uv}\mathrm{d}U/\mathrm{d}y$) peak at $y_* \approx 14$. Here u and v denote velocity fluctuations in the streamwise and wall-normal directions, respectively, and $\overline{uv}$, the Reynolds stress, is the temporal covariance. Of particular importance is the universal presence of 'streaks' in the wall region[8,9], which refer to counter-rotating rolls, aligned in the stream direction, that confer on the flow a (statistically) quasi-periodicity in the transverse direction of wavelength $\lambda \approx 100 l_*$ (ref. 10). ('Transverse' here indicates the direction across the width of the channel.) Simulations indicate that these are tubular structures, of positive or negative vorticity with respect to the stream, which extend in the stream direction for as much as $1{,}000 l_*$ (ref. 11). Simple scaling arguments suggest that roll spacing should grow linearly with wall-normal distance, and this has been verified experimentally[2]. A variety of mechanistic theories have been suggested to explain the presence of streaks[12–14], with no general agreement. More recently a statistical theory[15] suggests that the rolls are the result of an inverse cascade[16,17]; that is, instead of the normal cascade of turbulence to smaller scales, this cascade takes the flow to larger scales. The spacing is then well estimated by balancing turbulence production and the rate of ejected energy from the wall region.

It has long been known that these structures undergo a rapid cycle of events culminating in their eruption from the wall region, known as 'bursts', which results in slow-moving wall fluid entering the outer region and fast-moving outer fluid entering the wall region; the latter are known as 'sweeps'[18–20]. These relatively infrequent events account for a significant fraction of wall drag. One view of this phenomenon is that if coherent structures could be stabilized drag would be reduced. (Or from a more general perspective, stabilized coherent structures present a barrier to the cascade to small scales, and hence their maintained presence would impede the rate of energy loss.) Explanations of drag reduction by means of riblets use this viewpoint[21]. Riblets (wall grooves aligned with the stream, with transverse wavelength and height $\sim 15 l_*$), which in physical experiments can produce drag reductions of ~6% (refs 21, 22), and ~4% in simulations[23,24], are thought to restrain the movement of the rolls and therefore maintain their coherence. The methods of turbulence control presented here differ radically from this approach.

Analysis of several numerical simulations[25,26] reveals that turbulent energy resides primarily in stream-independent (roll) modes. Further, this analysis also revealed the presence of propagating plane

wave modes travelling downstream at an almost fixed speed. These are possibly related to the sublayer waves observed by Morrison *et al.*[27]. The waves, which are obliquely orientated with respect to the direction of flow, undergo triad interactions with the roll modes. The most intense of these interactions take place with waves which propagate in a range of angles, 45°–65°, to the right or left of the stream direction and have length scales comparable to the roll size. A recent numerical investigation (carried out in the simplifying framework of a minimal channel[28]) gives further evidence of the importance of the interaction between selected propagating modes and the energy-bearing roll modes for the cycle of events which occur in the flow[29]. (For a recent review see ref. 30.) The importance of these interactions has been further underlined in an earlier investigation in which the relevant propagating waves received regular phase randomization (a workless change) during the course of the simulation[31]. This numerical experiment led to drag reductions well in excess of 50%. This drag reduction is comparable to that found in low-concentration polymer additive experiments[32,33]; there was a close resemblance in all statistical measures for the case of polymers and the simulation.

This series of observations suggested that management of wall turbulence might be achieved with wall protrusions, chosen to excite appropriate propagating modes. This was tested in the channel shown in Fig. 1a; details are given in the figure legend. Of the variety of wall patterns that were tested, two are shown in Fig. 1b and c. Here we will focus on experiments performed on these two patterns, and comment briefly on other tested patterns.

The entrant flow passed through 157h of the channel (this includes the rough surface) before reaching the mid-station, B. Hot-wire measurements were taken at station B, and pressure measurements were made at the other stations shown in Fig. 1a. Channel geometry and Reynolds-number range are comparable to other reported experiments[34–36]. However, although our channel was significantly longer than in these other studies, it fell short of the length of the channel used by Hussain and Reynolds[37]. A small along-stream variation existed beyond B (see below), as implied by Hussain and Reynolds[37].

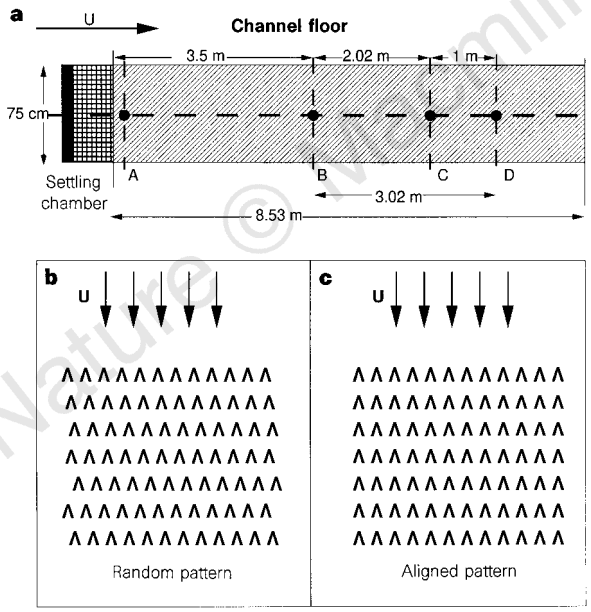

Figure 1 a, Plan view of the floor of the channel used in these experiments. The region shown black is 0.3 m long and represents the settling chamber into which flow enters vertically through 4-mm holes, both in the floor and the ceiling of the channel. The following 0.9 m (squares) is a rough surface. The remainder of the channel (hatched) is either covered with the patterns shown in **b** or **c**, or left smooth. The floor to ceiling height is 5.63 cm, whether the floor is covered with patterns or not. As the protrusions of the pattern, on average, effectively shorten the height, our measurements are conservative. (Surface area is increased by ~5%.) The black circles on the centre line show pressure-tap locations. The mid-station, B, houses a hot-wire system which yields wall-normal and transverse measurements. **b**, **c**, Protrusion patterns on channel floor. Pattern **b** is obtained from the regular array shown in **c** by random shifts of rows. Each vee has width in the transverse direction of 200/$_*$ period in the transverse direction of 260/$_*$ and period in the flow direction of 300/$_*$. The height of the vees, perpendicular to the floor, is 5/$_*$–6/$_*$.

A series of baseline measurements, for later comparison, were carried out in the absence of any applied patterns, and all mention of drag increase or decrease are relative to this baseline data set. Figure 2 shows the Reynolds-number ($= U_0 2h/\nu$) dependence of the unaveraged raw data for the friction coefficient C_f ($= 2u_*^2/U_0^2$). Individual data sets showed little noise and each is well fitted by a power law. The average over the four data sets conforms to the power law, $C_f \approx 0.0254/\mathrm{Re}^{0.165}$, which compares with $C_f \approx 0.0269/\mathrm{Re}^{0.178}$ found by Hussain and Reynolds, who averaged over many experiments performed over a significantly larger Reynolds-number range. (The four data sets shown in Fig. 2 are actually quite close; the lower two sets of points are fitted by $C_f \approx 0.0253/\mathrm{Re}^{0.167}$.) The vertical variation, $<\pm 3\%$, seen in the plot was due to uncontrollable ambient conditions. Transducer calibrations indicated a sensitivity of 0.5%, and pressure variations due to temperature changes caused a $\pm 0.8\%$ error, resulting in a net $\pm 1.3\%$ error in the friction measurements. Mean velocity and Reynolds stress measurements performed at B confirmed the friction values shown in Fig. 2. These and other turbulence statistics will be reported elsewhere.

Figure 2 also shows the results for C_f when the randomly shifted row pattern (Fig. 1b) is applied to the floor of the channel. C_f for the three data sets for the patterned floor all lie below their smooth-floor counterparts. The average of these, $C_f \approx 0.0248/\mathrm{Re}^{0.172}$, represents a drag reduction of ~10% against the smooth-floor average over the range shown. The peak drag reduction, data points represented by '×'s over the smooth-floor average, exceeds 12.5%. The C_f results shown in Fig. 2 and quoted here are based on pressure drops measured between B and D, a 3.02-m span. C_f, when measured between B and C, a 2.02-m span, differed by 2% from these values. Although this lies within experimental error we took it as an indication of residual stream dependence.

The pattern was chosen (on the basis of the above-cited references) to produce waves which interact maximally with the energy-bearing roll modes. The goal was to prevent formation of the rolls, and to break them up if formed. As a heuristic argument to support this strategy, we can suppose that roll structures have characteristic velocity u_0, and dimension λ_0. It might then be supposed that $\tau_0 = \lambda_0/u_0$ is characteristic of the duration of a burst. We denote by fu_0^2 the fraction of the energy contained in roll modes. Flow visualizations imply that as a consequence of a burst the roll goes directly into small scales; on these grounds fu_0^2/τ^0 is a measure of the dissipation rate due to the rolls. On the other hand, if instead the rolls were to follow the cascade route to dissipation, as forced by the protrusions, the estimate changes. We will now assume that the Kolmogorov spectrum is valid for scales below λ_0, that is, for $\lambda \leqslant \lambda_0$, $u^2/u_0^2 \propto (\lambda/\lambda_0)^{5/3}$ and therefore $\tau/\tau^0 \propto (\lambda/\lambda_0)^{1/6}$. To model the cascade we will regard an eddy as halving in size for each turnover time. Thus the time $\bar{\tau}$ to fully dissipate the eddy is $\bar{\tau}/\tau^0 = \Sigma_{n=0}^{\infty}(2^n)^{1/6}(1-2^{1/6})^{-1} \approx 8.3$. Thus within this crude depiction of the phenomena, energy degradation is delayed and therefore the dissipation rate due to rolls alone is substantially reduced. From this it can be inferred that the roll modes now carry less energy than in the standard smooth case. The principal premise of this simple modelling of events is that by preventing the creation of the roll 'coherent structures' we delay the time taken until the final loss to dissipation.

Additional measurements support this picture. Burst (and

sweep) frequency ω were measured at the upper (smooth) wall of the channel (the 'ceiling') and the lower (patterned) floor at a wall-normal distance of 30 l_* and centre-line velocity of 6 m s^{-1}. Following Alfredsson and Johansson[38], a burst at the channel ceiling is said to occur when $uv > 4u_{rms}v_{rms}$ and $v < 0$ (and a sweep when $v > 0$). Similarly for the channel floor, but for proper comparison the r.m.s. values at the ceiling are used. By these criteria we found the normalized burst frequency, $\omega h/U_0$, at the ceiling to be 0.127 which is comparable to value found in ref. 38. By comparison, the patterned floor had a significantly lower burst frequency of 0.050. (A comparable reduction in the sweep frequency also occurred.) Transverse correlation measurements indicated a streak spacing at the patterned wall 10% greater than at the smooth wall. Also, v_{rms} in the vicinity of the patterned wall was found to be less than at the smooth wall. Increased streak spacing and a diminished v_{rms} are consistent with drag reduction using trace amounts of polymer additives[32].

It has recently been shown that if contributions to the average Reynolds stress is separated into roll and propagating mode contributions[29], then roll modes are the major contributors near the wall, whereas propagating modes mainly contribute in the core. By interfering with the formation of the roll modes, as the protrusions do, we can diminish the contribution from roll modes.

We performed experiments designed to increase the fraction of energy which reside in roll modes. This was accomplished by using the pattern of protrusions shown in Fig. 1c. In this case, the same 'vee' protrusions (having the same height of roughly 5 l_*–6 l_*) are now aligned as columns in the stream direction. As evidenced from direct hot-wire spanwise transverse measurements, a statistically steady array of counter-rotating rolls was established. Thus, the energy in roll modes was increased. In this case a drag increase well in excess of 20% was obtained. The results are indicated in the upper part of Fig. 2. Unfortunately these data were acquired from pressure-tap locations still showing along-stream variation. As a consequence the results underestimate the effect.

The bursting of the rolls was facilitated by increasing their production. The simple change of misaligning or aligning of the vees, all of which point in the upstream direction, results in a drag reduction of >10% altering to a drag increase in excess of 20%. We have also tested the pattern shown Fig. 1c, but with alternate rows shifted a half-wavelength. This also produced a drag reduction but was less effective than the randomly slid rows of Fig. 1b. Variations in protrusion heights and the effect of the inclusion of additional permissible vee angles remain to be studied.

A straightforward argument indicates that if both floor and ceiling of the channel are covered with the patterned material, the effect should at least double. Unfortunately, the design of the channel did not allow this and we were not able to pursue this idea. We are redesigning the channel to permit such experiments. Finally, we mention that over the past 15 months, during which we improved our experimental procedures and verified the phenomena, almost without exception each experiment with the randomly patterned floor showed a drag reduction. □

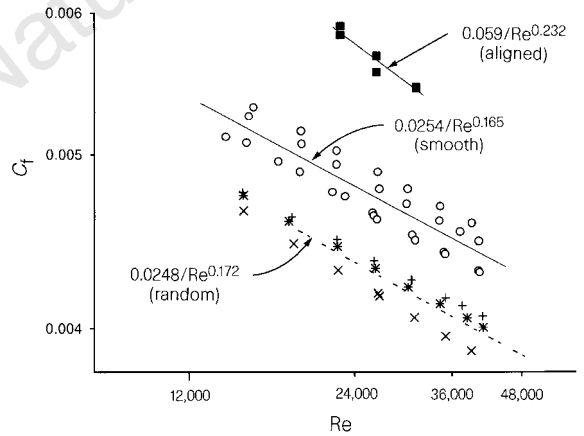

Figure 2 Plot of friction coefficient C_f (= $2u_*^2/U_0^2$) against Reynolds number Re (= $U_0 2h/\nu$). Circles, results of four independent experimental runs in a channel with a smooth floor. The continuous straight line is the regression fit to these data. The three sets of symbols in the lower portion of the plot represent three independent experimental runs with the random pattern of Fig. 1b on the floor of the channel. The dashed line is the result of a regression analysis on these data. The filled squares in the upper portion of the figure represent runs carried out on the aligned pattern shown in Fig. 1c. The analytic form of the regression fits are indicated by arrows.

Received 1 April 1997; accepted 1 July 1997.

1. Coustols, E. & Savill, A. M. in *AGARD FDP/VKI Special course on Skin Friction and Drag Reduction*. 2–6 March, VKI Brussels, Belgium (1992).
2. Rajaee, M., Karlsson, S. K. F. & Sirovich, L. On the streak spacing and vortex roll size in a turbulent channel flow. *Phys. Fluids* **258,** 2439–2443 (1995).
3. Patel, V. C. & Head, M. R. Some observations on skin friction and velocity profiles in developed pipe and channel flows. *J. Fluid Mech.* **38,** 181–193 (1969).
4. von Karman, T. Mechanische ahnlichkeit und turbulenz. *Nachr. Akad. Wiss. Göttingen* **58,** (1930).
5. Millikan, C. B. A. in *5th Int. Congr. of Applied Mechanics* 386 (Wiley, New York, 1938).
6. Zagarola, M. V. & Smits, A. J. Scaling of the mean velocity profiel for turbulent pipe flow. *Phys. Rev. Lett.* **78,** 239–242 (1997).
7. Zagarola, M. V., Perry, A. E. & Smits, A. J. Log laws or power laws: The scaling in the overlap region. *Phys. Fluids* **9,** 2094–2100 (1997).
8. Kline, S. J., Reynolds, W. C., Schraub, F. A. & Runstadler, P. W. The structure of turbulent boundary layers. *J. Fluid Mech.* **95,** 741–773 (1967).
9. Kim, H. T., Kline, S. J. & Reynolds, W. C. The production of turbulence near a smooth wall in a turbulent boundary layer. *J. Fluid Mech.* **50,** 133–160 (1971).
10. Smith, C. R. & Metzler, S. P. The characteristics of low-speed streaks in the near-wall region of a turbulent boundary layer. *J. Fluid Mech.* **129,** 27–54 (1983).
11. Bernard, P. S., Thomas, J. M. & Handler, R. A. Vortex dynamics and the production of Reynolds stress. *J. Fluid Mech.* **253,** 385–419 (1993).
12. Jang, P. S., Benney, D. J. & Gran, R. L. On the origin of streamwise vortices in a turbulent boundary layer. *J. Fluid Mech.* **169,** 109–123 (1986).
13. Butler, K. M. & Farrell, B. F. Optimal perturbations and streak spacing in wall-bounded turbulent shear flow. *Phys. Fluids* **5,** 774–777 (1993).
14. Waleffe, F. On a self-sustaining process in shear flows. *Phys. Fluids* **4,** 883–900 (1997).
15. Sirovich, L. Origin and spacing of streaks in wall bounded turbulence. *Phys. Fluids* (submitted).
16. Onsager, L. Statistical hydrodynamics. *Nuovo Cimento* **VI,** 279–287 (1949).
17. Kraichnan, R. H. Inertial ranges in two-dimensional turbulence. *Phys. Fluids* **10,** 1417–1423 (1967).
18. Offen, G. R. & Kline, S. J. Combined dye streak and hydrogen bubble visual observations of a turbulent boundary layer. *J. Fluid Mech.* **62,** 223–239 (1974).
19. Corino, E. R. & Brodkey, R. S. A visual investigation of the wall region in turbulent flow. *J. Fluid Mech.* **37,** 1–30 (1969).
20. Coles, D. E. in *Coherent Structure of Turbulent Boundary Layers* (eds Smith, C. R. & Abbot, D. E.) (AFOSR/Lehigh Univ. Workshop, Dept of Mech. Eng. Mech. Bethlehem, PA, 1978).
21. Walsh, M. J. in *Progress in Astronautics and Aeronautics* Vol. 123 (eds Bushnell, D. & Hefner, J.) (AIAA, Reston, VA, 1990).
22. Coustols, E. & Cousteix, J. in *Proc. 2nd IUTAM Symp. on Structure of Turbulence and Drag Reduction.*
23. Goldstein, D., Handler, R. & Sirovich, L. Direct numerical simulation of turbulent flow over a modeled riblet covered surface. *J. Fluid Mech.* **302,** 333–375 (1995).
24. Chu, D. c. & Karniadakis, G. E. The direct numerical simulation of laminar and turbulent flow over riblets. *J. Fluid Mech.* **250,** 1–42 (1993).
25. Sirovich, L., Ball, K. S. & Keefe, L. R. Plane waves and structures in turbulent channel flow. *Phys. Fluids* **2,** 2217–2226 (1990).
26. Sirovich, L., Ball, K. S. & Handler, R. A. Propagating structures in wall-bounded turbulent flows. *Theor. Comput. Fluid Dyn.* **2,** 307–317 (1991).
27. Morrison, W. R. B., Bullock, K. J. & Kronauer, R. E. Experimental evidence of waves in the sublayer. *J. Fluid Mech.* **47,** 639–656 (1971).
28. Jimenez, J. & Moin, P. The minimal flow unit in near-wall turbulence. *J. Fluid Mech.* **225,** 213–240 (1991).
29. Webber, G. A., Handler, R. A. & Sirovich, L. The Karhunen-Loeve decomposition of minimal channel flow. *Phys. Fluids* **9,** 1054–1066 (1997).
30. Sirovich, L. in *Self-Sustaining Mechanisms of Wall Turbulence* (ed. Panton, R. L.) (Computational Mechanics Publications, Southampton, in the press).
31. Handler, R. A., Levich, E. & Sirovich, L. Drag reduction in turbulent channel flow by phase randomization. *Phys. Fluids* **5,** 686 (1993).
32. Tiederman, W., Luchik, T. & Bogard, D. Wall-layer structure and drag reduction. *J. Fluid Mech.* **156,** 419–437 (1985).
33. Eckelman, L., Fortuna, G. & Hanratty, T. J. Drag reduction and wavelengths of flow-oriented wall eddies. *Nature* **236,** 94–96 (1972).
34. Laufer, J. The structure of turbulence in fully developed pipe flow. *Report* 1174 (Nat. Adv. Com. Aeronaut., Washington DC, 1954).
35. Clark, J. A. A study of incompressible turbulent boundary layers in channel flow. *Trans. ASME Ser. D* **90,** 445–455 (1968).
36. Comte-Bellot, G. *Ecoulement Turbulent Entre Deux Parois Paralleles* (Publications Scientifiques et Techniques Vol. 419, Minstere de L'air, Paris, 1965).
37. Hussain, A. K. M. F. & Reynolds, W. C. Measurements in fully developed turbulent channel flow. *J. Fluid Eng.* **97,** 568–580 (1975).
38. Alfredsson, P. H. & Johansson, A. V. Time scales in turbulent channel flow. *Phys. Fluids* **27,** 1974–1981 (1984).

Acknowledgements. We thank E. Levich for help in the initiation of the experiment; B. Knight for many discussions; M. Rajee for his contribution until he left in January 1996; R. Handler and D. Goldstein for calculations; U. Fisher (Ormat Industries) for preparation of the patterned materials; and Y. Bronicki for support and encouragement. This work was done in the framework of a project initiated and supported by Orlev Scientific/Ormat Industries Ltd, Yavne, Israel. Experimental facilities were provided under an agreement with Brown University.

Correspondence should be addressed to L.S. at the Laboratory of Applied Mathematics, Box 1012, CUNY/MSSM, New York, NY 10029-6574, USA (e-mail: chico@camelot.mssm.edu).